Stem Cell Reports
Report
OPEN ACCESS

BAK/BAX-Mediated Apoptosis Is a *Myc*-Induced Roadblock to Reprogramming

Esther J.Y. Kim,[1,2] Minna-Liisa Anko,[3] Christoffer Flensberg,[1,2] Ian J. Majewski,[1,2] Fan-Suo Geng,[1,2] Jaber Firas,[3] David C.S. Huang,[1,2] Mark F. van Delft,[1,2,4,*] and Joan K. Heath[1,2,4,*]
[1]The Walter and Eliza Hall Institute of Medical Research, 1G Royal Parade, Parkville, VIC 3052, Australia
[2]Department of Medical Biology, University of Melbourne, Parkville, VIC 3052, Australia
[3]Department of Anatomy and Developmental Biology, Biomedicine Discovery Institute, Development and Stem Cells Program, Monash University, Clayton, VIC 3800, Australia
[4]Co-senior author
*Correspondence: vandelft@wehi.edu.au (M.F.v.D.), joan.heath@wehi.edu.au (J.K.H.)
https://doi.org/10.1016/j.stemcr.2017.12.019

SUMMARY

Despite intensive efforts to optimize the process, reprogramming differentiated cells to induced pluripotent stem cells (iPSCs) remains inefficient. The most common combination of transcription factors employed comprises OCT4, KLF4, SOX2, and MYC (OKSM). If MYC is omitted (OKS), reprogramming efficiency is reduced further. Cells must overcome several obstacles to reach the pluripotent state, one of which is apoptosis. To directly determine how extensively apoptosis limits reprogramming, we exploited mouse embryonic fibroblasts (MEFs) lacking the two essential mediators of apoptosis, BAK and BAX. Our results show that reprogramming is enhanced in MEFs deficient in BAK and BAX, but only when MYC is part of the reprogramming cocktail. Thus, the propensity for *Myc* overexpression to elicit apoptosis creates a significant roadblock to reprogramming under OKSM conditions. Our results suggest that blocking apoptosis during reprogramming may enhance the derivation of iPSCs for research and therapeutic purposes.

INTRODUCTION

Reprogramming somatic cells to a pluripotent state can be achieved through ectopic expression of pluripotency transcription factors (Takahashi and Yamanaka, 2006). The resulting induced pluripotent stem cells (iPSCs) hold immense promise as tools for research and regenerative therapy. To harness their full potential, studies have scrutinized the molecular mechanisms underpinning reprogramming, and sought to identify factors able to improve this inherently inefficient process (Esteban et al., 2010; Onder et al., 2012). One well-characterized means of enhancing reprogramming is to inhibit the activity of TP53/TRP53 (hereafter, p53) (Hong et al., 2009; Kawamura et al., 2009; Marion et al., 2009; Utikal et al., 2009). The improved reprogramming efficiency of p53-deficient cells has been attributed to the ability of p53 to trigger senescence and apoptosis. While senescence has been confirmed as a major reprogramming barrier (Banito et al., 2009; Kawamura et al., 2009), the significance of mitochondrial apoptosis is less clear.

Mitochondrial apoptosis is a conserved intrinsic cell death program controlled by interactions between diverse members of the BCL2 protein family, of which there are three functional classes: the pro-survival BCL2-like proteins, the pro-apoptotic BH3-only proteins, and the apoptosis effector proteins, BAK and BAX (Figure S1). In healthy cells, the BCL2-like survival proteins suppress mitochondrial apoptosis by restraining BAK and BAX. However, in response to various forms of cellular stress, including cytokine deprivation, DNA damage, and oncogene activation, BH3-only proteins are triggered to initiate apoptosis both by inhibiting BCL2-like proteins and by directly activating BAK and BAX. Once activated, BAK and BAX oligomerize on the outer mitochondrial membrane to drive its rupture (Czabotar et al., 2013). The ensuing mitochondrial outer membrane permeabilization (MOMP) results in the efflux of pro-apoptogenic factors, including cytochrome *c*, to the cytosol. At this point, the cell is irreversibly committed to death, and a cascade of proteolytic caspases is activated that brings about the ordered demolition of cellular components.

Deciphering the role of apoptosis in cellular processes can be complicated by the fact that each of the three classes of BCL2 family proteins comprises multiple family members, and that each of these proteins has a certain propensity to interact with and regulate the others (Chen et al., 2005; Czabotar et al., 2014; Willis et al., 2007). As such, there is a large degree of functional overlap and redundancy within the family. Importantly for our studies, however, BAK and BAX are the only two BCL2 family members able to drive MOMP, and in their combined absence, the mitochondrial apoptosis pathway is completely abolished (Lindsten et al., 2000).

Thus far, attempts to resolve the role, if any, of mitochondrial apoptosis during reprogramming have primarily focused on upstream regulators, including BCL2, the archetypal pro-survival BCL2 family member, and PUMA, a p53-regulated BH3-only protein (Kawamura et al., 2009; Lake et al., 2012; Li et al., 2013). These studies have produced conflicting data, with two studies reporting

significant enhancement of reprogramming efficiency when apoptosis was blocked, either through BCL2 overexpression or PUMA depletion (Kawamura et al., 2009; Li et al., 2013), and another reporting that PUMA depletion promoted reprogramming under OKS but not OKSM conditions (Lake et al., 2012).

To directly evaluate the influence of apoptosis on the efficiency of reprogramming, we used mouse embryonic fibroblasts (MEFs) lacking both BAK and BAX. Such cells provide a definitive model system in which to study cellular processes in the absence of mitochondrial apoptosis (Lindsten et al., 2000). Here, we report that *Bak*$^{-/-}$;*Bax*$^{-/-}$ MEFs undergo reprogramming with markedly increased efficiency compared with their wild-type (WT) counterparts in OKSM, but not OKS conditions. Remarkably, they traverse this process without incurring significantly increased genomic instability. Our data conclusively demonstrate that mitochondrial apoptosis imposes a strong barrier to OKSM-mediated iPSC induction, and that this roadblock is MYC-dependent. While the overall efficiency of iPSC derivation is markedly improved with ectopic *Myc* expression, the heightened sensitivity to apoptosis curtails its full benefit in reprogramming.

RESULTS AND DISCUSSION

Mitochondrial Apoptosis: A Barrier to iPSC Derivation by OKSM Expression

To examine the role of mitochondrial apoptosis in reprogramming, WT and *Bak*$^{-/-}$;*Bax*$^{-/-}$ MEFs were transduced with lentiviral OKSM factors. After 18 days of reprogramming, *Bak*$^{-/-}$;*Bax*$^{-/-}$ MEFs yielded alkaline phosphatase (AP)-positive colonies (Figure 1A) that were morphologically indistinguishable from those derived from WT MEFs (Figure S2A). Moreover, they displayed markedly improved reprogramming efficiency compared with WT MEFs, as measured by AP activity (Figure 1B) and verified by immunocytochemical staining of the pluripotency marker, NANOG (Figure S2B). Meanwhile, deficiency in either BAK or BAX alone did not significantly affect the yield of AP-positive colonies (Figures 1A and 1B). This is consistent with their functional redundancy in mediating MOMP, and proves that the increased reprogramming efficiency of *Bak*$^{-/-}$;*Bax*$^{-/-}$ MEFs is attributable to attenuation of mitochondrial apoptosis.

To further assess the pluripotency of colonies generated from *Bak*$^{-/-}$;*Bax*$^{-/-}$ MEFs, we cultured them over at least five passages to confirm their self-renewal capacity, during which time they maintained a shiny, rounded morphology and expression of the pluripotency markers SSEA1, NANOG, and OCT4 (Figure 1C). These observations are consistent with those reported for embryonic stem cells deficient in BAK and BAX (Wang et al., 2015).

Next, to assess the differentiation capacity of *Bak*$^{-/-}$;*Bax*$^{-/-}$ iPSCs, we generated embryoid bodies by the hanging drop method. Cells from three independent lines spontaneously differentiated into cells representative of all three germ layers (Figure 1D). Finally, we investigated the *in vivo* differentiation capacity of the *Bak*$^{-/-}$;*Bax*$^{-/-}$ iPSC lines by injecting them subcutaneously into mice. The resulting teratomas contained tissues derived from all three germ layers (Figure 1E).

Elevated Caspase-3/7 Activity during OKSM Reprogramming Suggests MYC-Stimulated Apoptosis Forms a Significant Barrier to Reaching Pluripotency

Having observed that *Bak*$^{-/-}$;*Bax*$^{-/-}$ MEFs reprogrammed more efficiently upon the expression of OKSM factors, we next tested whether this would also hold true when MEFs were reprogrammed without MYC, given its propensity to promote apoptosis. When MEFs were reprogrammed with only OKS, there was a striking decrease in iPSC formation compared with MEFs reprogrammed with OKSM (Figure 2A), consistent with previous reports (Nakagawa et al., 2008). However, there was no significant difference in reprogramming efficiencies between *Bak*$^{-/-}$;*Bax*$^{-/-}$ and WT cultures (Figure 2A); this suggests that in the absence of ectopic MYC expression, apoptosis does not significantly limit reprogramming. Conversely, we hypothesize that ectopic MYC expression drives elevated levels of apoptosis that in turn limits the efficiency of OKSM reprogramming.

To determine whether apoptosis was indeed elevated during OKSM relative to OKS reprogramming, we measured caspase-3/7 activity over the first 12 days of reprogramming using the Caspase-Glo 3/7 Assay System (Promega). To establish a reference for these assays, we induced apoptosis in 100% of MEFs by treating them with small molecule inhibitors of the pro-survival proteins, MCL1 (S63845; Kotschy et al., 2016) and BCLXL for 6 hr (A-1331,852; Leverson et al., 2015). As expected, robust caspase-3/7 activity was elicited in WT but not *Bak*$^{-/-}$;*Bax*$^{-/-}$ MEFs (Figure 2B). WT MEF cultures reprogrammed with OKSM exhibited elevated caspase-3/7 activity that peaked at approximately 10% of the level observed in the apoptotic reference sample (Figure 2C). Furthermore, caspase-3/7 activity was consistently higher in WT MEFs reprogrammed with OKSM compared with OKS throughout the duration of the experiment (Figure 2C). In contrast, we detected very low caspase-3/7 activity in reprogramming *Bak*$^{-/-}$;*Bax*$^{-/-}$ MEFs (Figures 2B and 2C).

These data are consistent with prior findings that ectopic MYC expression sensitizes cells to apoptosis (McMahon, 2014; Pelengaris et al., 2002) and lead us to conclude that mitochondrial apoptosis constitutes a major barrier to reprogramming when MYC is included as one of the pluripotency factors (Figure 2D). Thus, while MYC enhances

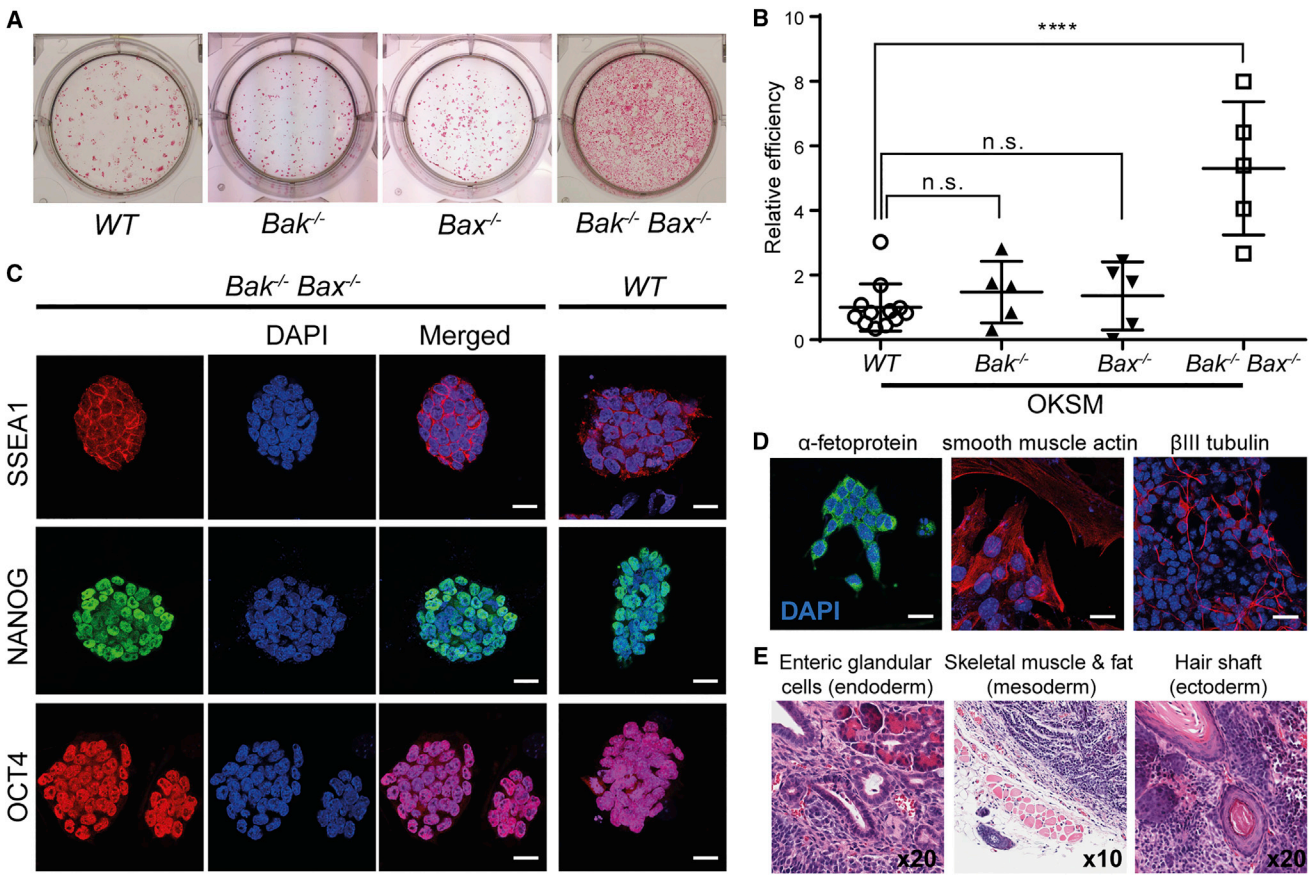

Figure 1. Enhanced Production of iPSCs in the Absence of Apoptosis Yields Fully Pluripotent Cells

(A) Alkaline phosphatase (AP) staining of WT, *Bak*$^{-/-}$, *Bax*$^{-/-}$, and *Bak*$^{-/-}$;*Bax*$^{-/-}$ MEFs at 18 days post transduction with OKSM reveals enhanced reprogramming efficiency in *Bak*$^{-/-}$;*Bax*$^{-/-}$ cells.

(B) Quantification of AP-positive colonies generated by each genotype relative to WT. Values shown are mean ± SD. ****$p < 0.0001$, $n \geq 5$ independent experiments, each with an independently derived MEF line. n.s., not significant.

(C) Expression of the pluripotency markers SSEA1, NANOG, and OCT4 in independent *Bak*$^{-/-}$, *Bax*$^{-/-}$ iPSC colonies passaged at least five times. During this time, the colonies maintained a characteristic iPSC morphology (see also Figure S2).

(D) *Bak*$^{-/-}$;*Bax*$^{-/-}$ embryoid bodies were produced from isolated iPSCs by the hanging drop method. These were cultured on adhesive surfaces for 2 weeks prior to staining for differentiation markers representing the three germ layers: α1 fetoprotein (endoderm), α smooth muscle actin (mesoderm), and βIII tubulin (ectoderm).

(E) Hematoxylin and eosin-stained sections of *Bak*$^{-/-}$;*Bax*$^{-/-}$ iPSC-derived teratomas reveals differentiated tissues representative of all three germ layers.

Scale bars, 20 μm.

overall reprogramming efficiency through reinforcing cell proliferation and growth, this is mitigated in part by an increase in BAK/BAX-mediated apoptosis.

p53-Mediated Apoptosis Is Not a Major Barrier to OKS Reprogramming

Previous studies have established p53 as a barrier to both OKSM and OKS-mediated reprogramming. While p53 drives a variety of cellular responses, it is primarily thought to hinder iPSC derivation by provoking senescence and apoptosis. Based on our observations that apoptosis was not a major barrier to OKS-mediated reprogramming (Figure 2A), we reasoned that deficiency of BAK and BAX would add little further advantage to *p53*-deficient cultures in OKS conditions. To test this, we introduced *p53* mutations in primary MEFs using CRISPR/Cas9 targeting. Western blots confirmed that single-guide RNAs (sgRNAs) targeting either exon 4 or exon 5 of *p53* were highly effective at ablating *p53* expression (Figure 3A; Aubrey et al., 2015). When reprogrammed with OKS, WT and *Bak*$^{-/-}$;*Bax*$^{-/-}$ MEFs expressing Cas9 together with sgRNA targeting *p53* both formed AP-positive iPSCs more efficiently than controls

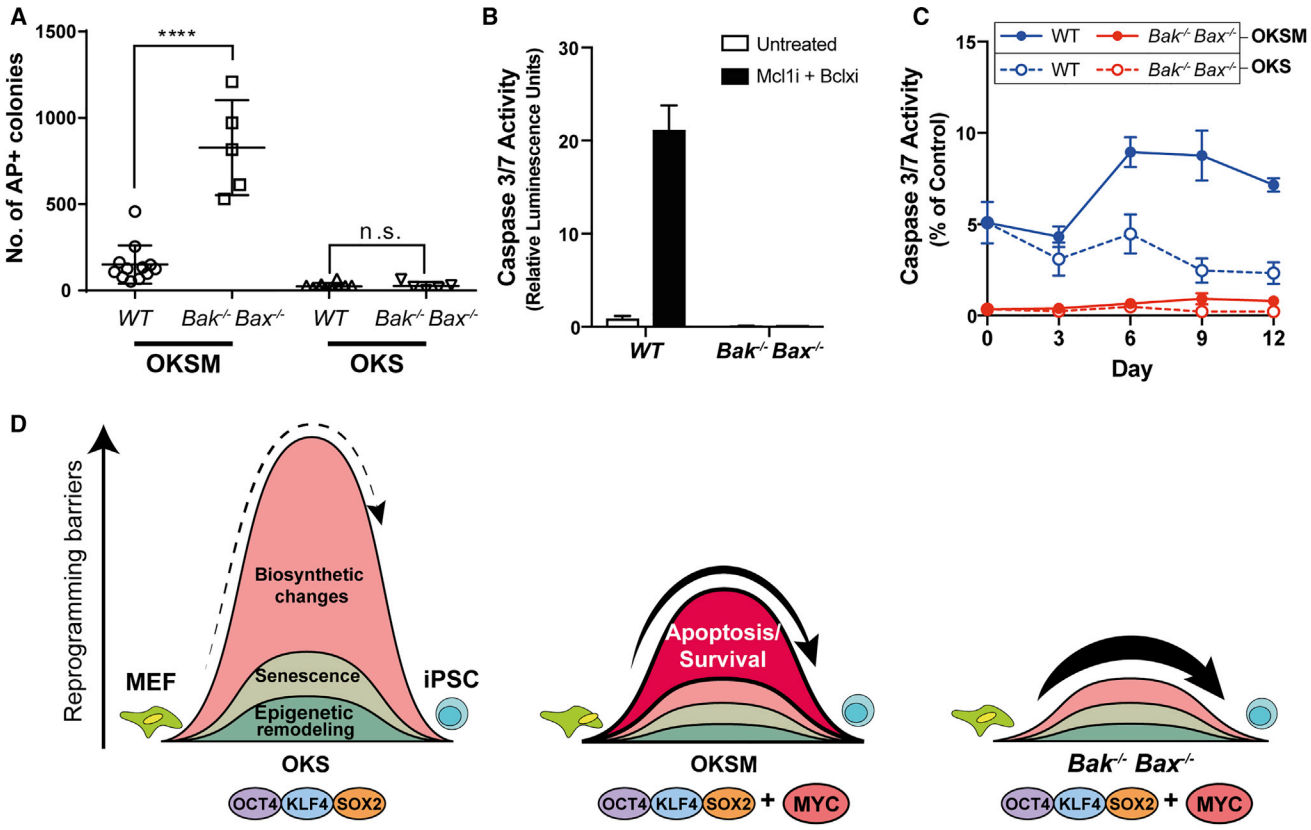

Figure 2. Apoptosis Is a *Myc*-Induced Reprogramming Roadblock

(A) *Bak*$^{-/-}$;*Bax*$^{-/-}$ MEFs transduced with OKSM produced significantly more AP-positive colonies compared with WT MEFs. In OKS conditions, WT and *Bak*$^{-/-}$;*Bax*$^{-/-}$ MEFs produced significantly fewer colonies, and there was no significant difference (n.s.) between them.

(B) WT and *Bak*$^{-/-}$;*Bax*$^{-/-}$ MEFs were treated for 6 hr with S63845 and A-1331852 to inhibit the pro-survival factors, MCL1 and BCLx, respectively. At this point, all WT cells exhibited high caspase-3/7 activity. In contrast, *Bak*$^{-/-}$;*Bax*$^{-/-}$ MEFs exhibited negligible caspase-3/7 activity, even in the presence of S63845 and A-1331852.

(C) Caspase-3/7 assays were conducted every 3 days during the first 12 days of reprogramming in OKSM and OKS conditions. WT MEFs transduced with OKSM factors exhibited significantly higher caspase-3/7 activity compared with WT MEFs transduced with OKS. Meanwhile, *Bak*$^{-/-}$;*Bax*$^{-/-}$ MEFs exhibited very low caspase-3/7 activity throughout the experiment, independently of whether they were transduced with OKSM or OKS.

(D) Proposed model: exogenous MYC enhances reprogramming by inducing biosynthetic changes favorable to reprogramming, including increased transcription, translation, and a switch from oxidative phosphorylation to a glycolytic mode of energy production. However, exogenous MYC also raises an apoptosis barrier, which is abolished in *Bak*$^{-/-}$;*Bax*$^{-/-}$ cells.

Values are mean ± SD, ****p < 0.0001, n ≥ 5 independent experiments, each with an independently derived MEF line.

expressing only Cas9 (Figure 3B). However, we observed no significant difference between the reprogramming capacity of WT or *Bak*$^{-/-}$;*Bax*$^{-/-}$ MEFs in the absence of p53 (Figure 3B). This confirms that when mitochondrial apoptosis is blocked in OKS conditions, other p53-driven responses, such as senescence, are likely to pose the primary reprogramming roadblocks.

Genomic Integrity of *Bak*$^{-/-}$;*Bax*$^{-/-}$ iPSCs Is Comparable with that of WT iPSCs

Apoptosis is sometimes regarded as a mechanism to safeguard genome integrity. A block in mitochondrial apoptosis might therefore have deleterious effects on genomic integrity during reprogramming. To investigate this, we examined DNA double-strand breaks and copy number alterations (CNAs) in several independent *Bak*$^{-/-}$;*Bax*$^{-/-}$ iPSC lines that had been propagated for two or more passages. Using γH2AX as a marker, we quantified DNA double-strand breaks and found no significant difference between WT and *Bak*$^{-/-}$;*Bax*$^{-/-}$ iPSC lines (Figures 4A and 4B). Furthermore, using low pass whole genome sequencing, we observed no significant difference in the number of CNAs in iPSC clones derived from *Bak*$^{-/-}$;*Bax*$^{-/-}$ MEFs compared with those derived from

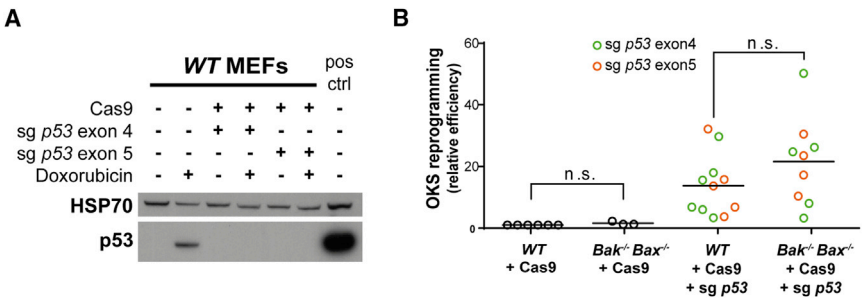

Figure 3. p53-Mediated Apoptosis Is Not a Barrier to OKS Reprogramming

(A) Western blot of p53 protein in primary MEFs expressing Cas9 and sgRNAs targeting either exon 4 or 5 confirms *p53* knockout in both examples. Cells were treated with doxorubicin to increase p53 protein to detectable levels. In the final lane, transformed MEFs overexpressing p53 were used as a positive control.

(B) WT *and* $Bak^{-/-}$;$Bax^{-/-}$ MEFs expressing Cas9 alone or together with sgRNA targeting *p53* were reprogrammed with OKS for 18 days, at which point AP-positive colonies were enumerated. The data are presented as efficiency relative to the WT-Cas9 control in each experiment. Bars represent the mean values for $n \geq 3$ independent experiments, each with an independently derived MEF line. n.s., not significant.

WT MEFs (Figures 4C, 4D, S3A, and S3B). Although this method is not sensitive enough to detect single-nucleotide aberrations that may occur during reprogramming, these results are consistent with reports that the process of reprogramming is not inherently mutagenic (Young et al., 2012) and that embryonic stem cells lacking BAK and BAX maintain a normal karyotype (Wang et al., 2015). In contrast, iPSC clones derived from *p53*-deficient MEFs exhibited a significantly higher number of CNAs compared with the $Bak^{-/-}$;$Bax^{-/-}$ and WT groups (Figures 4C, 4D, and S3C). In summary, MEFs unable to execute mitochondrial apoptosis display enhanced reprogramming capacity with OKSM without notable changes in genome stability.

Conclusion

Our observations lead us to conclude that MYC-driven BAK/BAX-mediated mitochondrial apoptosis presents a significant roadblock to OKSM reprogramming. While the overall effect of forced MYC expression favors reprogramming by regulating a broad range of biosynthetic processes required for enhanced cell growth and proliferation, including transcription, translation, and energy production (Nie et al., 2012; Polo et al., 2012; Sridharan et al., 2009), its propensity to sensitize cells to mitochondrial apoptosis partly mitigates these advantages (Figure 2D). In our hands, inhibiting apoptosis in $Bak^{-/-}$;$Bax^{-/-}$ iPSCs does not compromise their capacity to differentiate into lineages derived from all three germ layers, both *in vitro* and *in vivo*, nor have an adverse effect on genome integrity.

In conclusion, our study shows that harnessing the reprogramming-enhancing effects of MYC while selectively inhibiting its apoptotic response may be a useful strategy for efficient generation of iPSCs. We predict that studies aimed at improving our understanding of reprogramming factor stoichiometry and the specific downstream effectors of MYC will most likely make important contributions to improved iPSC derivation and application in the future.

EXPERIMENTAL PROCEDURES

Mouse Embryonic Fibroblasts

$Bak^{-/-}$ mice (gift of Craig Thompson; Lindsten et al., 2000), $Bax^{-/-}$ mice (Jackson Laboratory; Knudson et al., 1995) were backcrossed to C57BL/6 mice for >10 generations, then inter-crossed to generate $Bak^{-/-}$;$Bax^{-/-}$ double-knockout (DKO) E13.5 embryos to obtain MEFs. WT MEFs were derived from C57BL/6 mice. $p53^{-/-}$ MEFs (Jacks et al., 1994) were a gift of Anne Voss. All procedures performed on mice were reviewed and approved by the Animal Ethics Committee of the Walter and Eliza Hall Institute of Medical Research.

Generation of MEFs Containing *p53* Mutations for OKS Reprogramming

MEFs were transduced with a lentivirus encoding doxycycline-inducible mCherry-Cas9 either alone or together with lentiviruses encoding a GFP expression marker and sgRNA targeting either exon 4 or 5 of *p53* (Aubrey et al., 2015). mCherry positive or mCherry/GFP double-positive cells were then sorted on a BD FACSAria III, and treated with doxycycline (2 μg/mL) for 48 hr before reprogramming.

Generation of Lentiviruses

HEK293T cells were plated at a density of 3×10^6 cells/9 cm plate the day prior to transfection. Plasmids encoding lentiviral packaging components, the ecotropic envelope glycoprotein, and the reprogramming cassette OKSM (Sommer et al., 2009) or OKS (Chang et al., 2009) were introduced into HEK293T cells with FuGENE 6 Transfection Reagent (Promega) according to the manufacturer's instructions. The medium was replaced 24 hr post transfection. Viral supernatants were collected from cells at 48 and 72 hr post transfection, filtered (0.45 μm), and added to MEFs alongside polybrene (5 μg/mL).

Mitochondrial Apoptosis Assay

At 3-day intervals following transduction of MEFs with OKS or OKSM, we collected, pooled, and lysed adherent and non-adherent cells in PBS containing NP-40 (1%). Protein content was quantitated with a BCA assay, and caspase activity was measured with the Caspase-Glo 3/7 Assay System (Promega). Luminescence

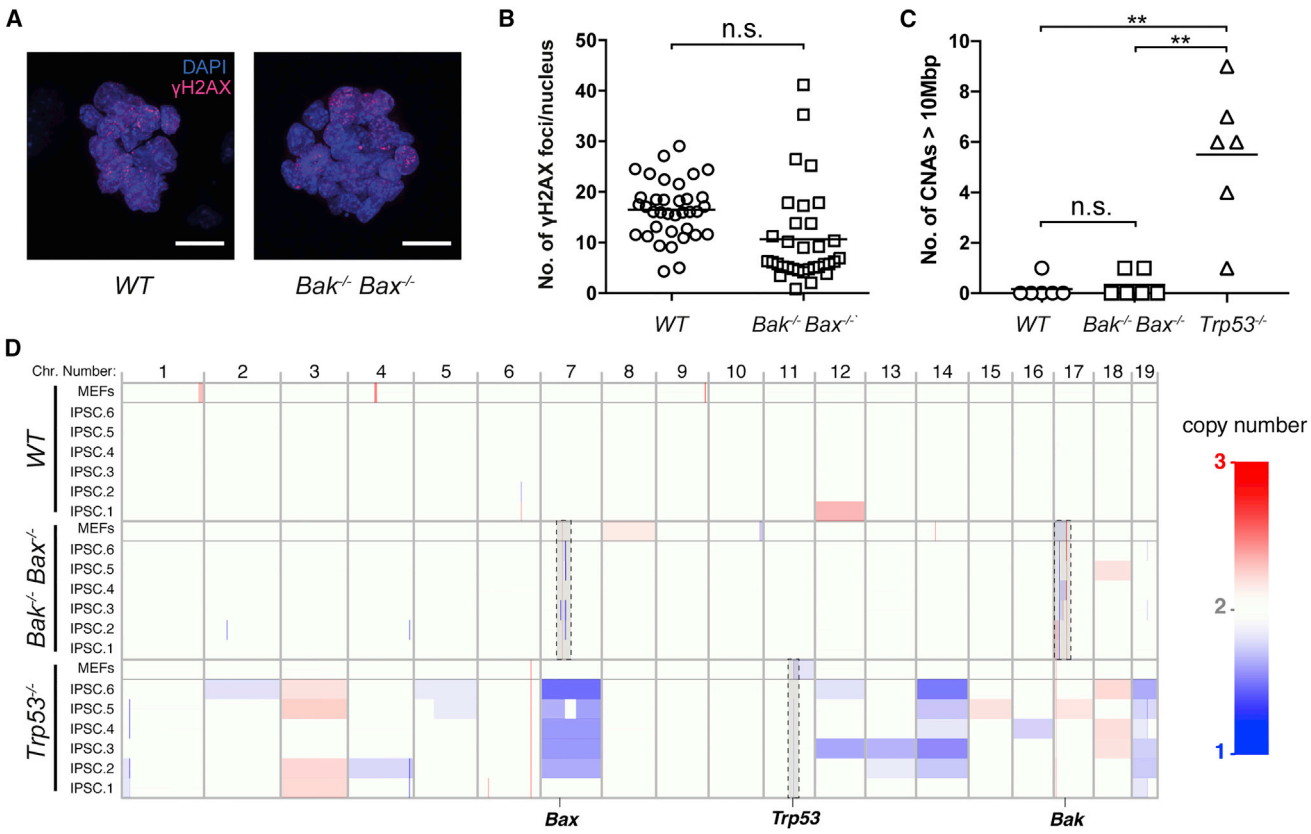

Figure 4. Enhanced Production of iPSCs in the Absence of Apoptosis Yields Cells with DNA and Genome Stability Comparable with that of WT iPSCs

Manually picked iPSC clones were cultured prior to assessment of genomic stability.

(A) Representative confocal images of iPSC colonies (passage 5) stained for γH2AX, which marks DNA double-strand breaks. Scale bars, 20 μm.

(B) Quantification of γH2AX foci was automated using γ-irradiated iPSC colonies as a positive control to set the threshold for fluorescence intensity. The average number of γH2AX foci in the nuclei of WT and *Bak*$^{-/-}$;*Bax*$^{-/-}$ iPSCs is not significantly different. For this experiment, independent MEF lines derived from different embryos (n = 4 for WT; n = 3 for *Bak*$^{-/-}$;*Bax*$^{-/-}$) were reprogrammed and corresponding iPSC lines established. Each point represents analysis of 1 colony (15–30 nuclei), with 9–12 colonies analyzed per independently derived iPSC line. Bars represent the mean values for each genotype. n.s., not significant.

(C) Quantification of CNAs in iPSC clones (passage 2) derived from *Bak*$^{-/-}$;*Bax*$^{-/-}$ MEFs compared with those derived from WT and *p53*$^{-/-}$ MEFs. There is no significant difference in the number of CNAs in WT and *Bak;Bax* DKO parental MEFs and their clonal iPSC derivatives. In contrast, iPSC clones derived from *p53*$^{-/-}$ MEFs exhibit a significantly higher number of CNAs (n = 6 iPSC clones derived from a single MEF line/genotype). Bars represent the mean values for each genotype. **p < 0.01, Mann-Whitney *U* test.

(D) A heatmap detailing CNAs on autosomal chromosomes (1–19, labeled at top) in MEF and clonal iPSC derivatives. Copy number is shown with a color scale, ranging from one to three copies (from blue to red). The genomic position of targeted genes is indicated along the bottom, and these loci are highlighted in the relevant samples (dashed boxes). See also Figure S3.

readings were divided by the protein content of the lysate to give a measure of caspase activity per milligram of protein, thereby correcting for the increase in cell number over the duration of the assay. To provide a positive control, we treated WT MEFs with S63845 (SYNthesis Med Chem) and A-1331852 (kind gift of Jean-Marc Garnier and Guillaume Lessene) to specifically inhibit two pro-survival Bcl2 family molecules, MCL1 and BCLx, respectively. This treatment produced synchronous apoptosis, which was morphologically evident in 100% cells after 6 hr. We designated the corresponding luminescence as the maximum expected value from the assay if all cells undergo apoptosis. Thus, at day 6, when WT-OKSM values peak at ~10% of this value, we extrapolated this to mean that ~10% of cells in the culture are apoptotic.

Detection of CNAs

Colonies of WT, *Bak*$^{-/-}$;*Bax*$^{-/-}$, and *p53*$^{-/-}$ iPSCs were picked and propagated for two passages. Genomic DNA was isolated from six clones of each genotype, plus the corresponding MEFs from which the clones were derived, using a DNeasy blood and tissue kit

(Qiagen). Libraries were prepared from sheared genomic DNA (~300 bp; 4 ng per sample) using a Truseq DNA sample preparation kit (Illumina). All 21 samples were applied to one lane of a NextSeq run, yielding ~4 million × 81 bp paired-end reads per library. Reads were aligned to *mm10* with BWA 0.7.15-r1140 (Li and Durbin, 2009) and analyzed with superFreq 0.9.21 (https://github.com/ChristofferFlensburg/superFreq) over 100 kbp bins, with increased sensitivity for CNAs with systematic variance set to 0.01. Limma-voom was used to estimate log fold change (LFC) and variance, which forms the input to a hierarchical segmentation of the genome. SuperFreq calls CNAs by comparing with a set of reference samples, which in this case comprised the WT colonies. When analyzing individual WT colonies, we compared them with a reference pool that included all other WT samples (i.e., the test sample was excluded from the reference pool). Using the superFreq calls, we counted copy number segments with an absolute LFC larger than 7% stretching over at least 10 Mbp.

Statistical Analysis

Graphs and p values were obtained with GraphPad Prism 6. Pairwise comparisons were made using Student's t test.

SUPPLEMENTAL INFORMATION

Supplemental Information includes Supplemental Experimental Procedures, three figures, and two tables and can be found with this article online at https://doi.org/10.1016/j.stemcr.2017.12.019.

AUTHOR CONTRIBUTIONS

E.J.Y.K. designed and conducted experiments, collected and assembled data, analyzed and interpreted data, wrote the paper, and approved the final manuscript. M.-L.A. designed and conducted experiments, analyzed and interpreted data, provided study materials, edited the paper, and approved the final manuscript. C.F. designed and conducted experiments, collected and assembled data, analyzed and interpreted data, edited the paper, and approved the final manuscript. I.J.M. designed experiments, provided study materials, analyzed and interpreted data, read the paper, and approved the final manuscript. F.-S.G. conducted experiments, read the paper, and approved the final manuscript. J.F. conducted experiments, read the paper, and approved the final manuscript. D.C.S.H. conceived and designed experiments, provided financial support and study materials, analyzed and interpreted data, edited the paper, and approved the final manuscript. M.F.v.D. designed and conducted experiments, provided study materials, collected and assembled data, analyzed and interpreted data, wrote the paper, and approved the final manuscript. J.K.H. conceived and designed experiments, provided financial support and study materials, analyzed and interpreted data, wrote the paper, and approved the final manuscript.

ACKNOWLEDGMENTS

We thank Sue Mei Lim for assistance with teratoma formation assays, Siddhartha Deb for pathological analysis, Jose Polo for discussions, Marco Herold for the validated *Cas9* and guide RNA constructs, and Lachlan Whitehead and Stephen Mieruszynski for image analysis. This research was supported by the Australian National Health and Medical Research Council (1043092, 1022870, 487922) and Ludwig Cancer Research, with operational infrastructure grants from the Australian Federal Government (IRISS) and the Victorian State Government (OIS).

Received: September 16, 2016
Revised: December 21, 2017
Accepted: December 21, 2017
Published: January 18, 2018

REFERENCES

Aubrey, B.J., Kelly, G.L., Kueh, A.J., Brennan, M.S., O'Connor, L., Milla, L., Wilcox, S., Tai, L., Strasser, A., and Herold, M.J. (2015). An inducible lentiviral guide RNA platform enables the identification of tumor-essential genes and tumor-promoting mutations in vivo. Cell Rep. *10*, 1422–1432.

Banito, A., Rashid, S.T., Acosta, J.C., Li, S., Pereira, C.F., Geti, I., Pinho, S., Silva, J.C., Azuara, V., Walsh, M., et al. (2009). Senescence impairs successful reprogramming to pluripotent stem cells. Genes Dev. *23*, 2134–2139.

Chang, C.W., Lai, Y.S., Pawlik, K.M., Liu, K., Sun, C.W., Li, C., Schoeb, T.R., and Townes, T.M. (2009). Polycistronic lentiviral vector for "hit and run" reprogramming of adult skin fibroblasts to induced pluripotent stem cells. Stem Cells *27*, 1042–1049.

Chen, L., Willis, S.N., Wei, A., Smith, B.J., Fletcher, J.I., Hinds, M.G., Colman, P.M., Day, C.L., Adams, J.M., and Huang, D.C. (2005). Differential targeting of prosurvival Bcl-2 proteins by their BH3-only ligands allows complementary apoptotic function. Mol. Cell *17*, 393–403.

Czabotar, P.E., Lessene, G., Strasser, A., and Adams, J.M. (2014). Control of apoptosis by the BCL-2 protein family: implications for physiology and therapy. Nat. Rev. Mol. Cell Biol. *15*, 49–63.

Czabotar, P.E., Westphal, D., Dewson, G., Ma, S., Hockings, C., Fairlie, W.D., Lee, E.F., Yao, S., Robin, A.Y., Smith, B.J., et al. (2013). Bax crystal structures reveal how BH3 domains activate Bax and nucleate its oligomerization to induce apoptosis. Cell *152*, 519–531.

Esteban, M.A., Wang, T., Qin, B., Yang, J., Qin, D., Cai, J., Li, W., Weng, Z., Chen, J., Ni, S., et al. (2010). Vitamin C enhances the generation of mouse and human induced pluripotent stem cells. Cell Stem Cell *6*, 71–79.

Hong, H., Takahashi, K., Ichisaka, T., Aoi, T., Kanagawa, O., Nakagawa, M., Okita, K., and Yamanaka, S. (2009). Suppression of induced pluripotent stem cell generation by the p53-p21 pathway. Nature *460*, 1132–1135.

Jacks, T., Remington, L., Williams, B.O., Schmitt, E.M., Halachmi, S., Bronson, R.T., and Weinberg, R.A. (1994). Tumor spectrum analysis in p53-mutant mice. Curr. Biol. *4*, 1–7.

Kawamura, T., Suzuki, J., Wang, Y.V., Menendez, S., Morera, L.B., Raya, A., Wahl, G.M., and Izpisua Belmonte, J.C. (2009). Linking the p53 tumour suppressor pathway to somatic cell reprogramming. Nature *460*, 1140–1144.

Knudson, C.M., Tung, K.S., Tourtellotte, W.G., Brown, G.A., and Korsmeyer, S.J. (1995). Bax-deficient mice with lymphoid hyperplasia and male germ cell death. Science *270*, 96–99.

Kotschy, A., Szlavik, Z., Murray, J., Davidson, J., Maragno, A.L., Le Toumelin-Braizat, G., Chanrion, M., Kelly, G.L., Gong, J.N., and Moujalled, D.M. (2016). The MCL1 inhibitor S63845 is tolerable and effective in diverse cancer models. Nature *538*, 477–482.

Lake, B.B., Fink, J., Klemetsaune, L., Fu, X., Jeffers, J.R., Zambetti, G.P., and Xu, Y. (2012). Context-dependent enhancement of induced pluripotent stem cell reprogramming by silencing Puma. Stem Cells *30*, 888–897.

Leverson, J.D., Phillips, D.C., Mitten, M.J., Boghaert, E.R., Diaz, D., Tahir, S.K., Belmont, L.D., Nimmer, P., Xiao, Y., Max Ma, X., et al. (2015). Exploiting selective BCL-2 family inhibitors to dissect cell survival dependencies and define improved strategies for cancer therapy. Sci. Transl. Med. *7*, 279ra40.

Li, H., and Durbin, R. (2009). Fast and accurate short read alignment with Burrows-Wheeler transform. Bioinformatics *25*, 1754–1760.

Li, Y., Feng, H., Gu, H., Lewis, D.W., Yuan, Y., Zhang, L., Yu, H., Zhang, P., Cheng, H., Miao, W., et al. (2013). The p53-PUMA axis suppresses iPSC generation. Nat. Commun. *4*, 2174.

Lindsten, T., Ross, A.J., King, A., Zong, W.X., Rathmell, J.C., Shiels, H.A., Ulrich, E., Waymire, K.G., Mahar, P., Frauwirth, K., et al. (2000). The combined functions of proapoptotic Bcl-2 family members bak and bax are essential for normal development of multiple tissues. Mol. Cell *6*, 1389–1399.

Marion, R.M., Strati, K., Li, H., Murga, M., Blanco, R., Ortega, S., Fernandez-Capetillo, O., Serrano, M., and Blasco, M.A. (2009). A p53-mediated DNA damage response limits reprogramming to ensure iPS cell genomic integrity. Nature *460*, 1149–1153.

McMahon, S.B. (2014). MYC and the control of apoptosis. Cold Spring Harb. Perspect. Med. *4*, a014407.

Nakagawa, M., Koyanagi, M., Tanabe, K., Takahashi, K., Ichisaka, T., Aoi, T., Okita, K., Mochiduki, Y., Takizawa, N., and Yamanaka, S. (2008). Generation of induced pluripotent stem cells without Myc from mouse and human fibroblasts. Nat. Biotechnol. *26*, 101–106.

Nie, Z., Hu, G., Wei, G., Cui, K., Yamane, A., Resch, W., Wang, R., Green, D.R., Tessarollo, L., Casellas, R., et al. (2012). c-Myc is a universal amplifier of expressed genes in lymphocytes and embryonic stem cells. Cell *151*, 68–79.

Onder, T.T., Kara, N., Cherry, A., Sinha, A.U., Zhu, N., Bernt, K.M., Cahan, P., Marcarci, B.O., Unternaehrer, J., Gupta, P.B., et al. (2012). Chromatin-modifying enzymes as modulators of reprogramming. Nature *483*, 598–602.

Pelengaris, S., Khan, M., and Evan, G. (2002). c-MYC: more than just a matter of life and death. Nat. Rev. Cancer *2*, 764–776.

Polo, J.M., Anderssen, E., Walsh, R.M., Schwarz, B.A., Nefzger, C.M., Lim, S.M., Borkent, M., Apostolou, E., Alaei, S., Cloutier, J., et al. (2012). A molecular roadmap of reprogramming somatic cells into iPS cells. Cell *151*, 1617–1632.

Sommer, C.A., Stadtfeld, M., Murphy, G.J., Hochedlinger, K., Kotton, D.N., and Mostoslavsky, G. (2009). Induced pluripotent stem cell generation using a single lentiviral stem cell cassette. Stem Cells *27*, 543–549.

Sridharan, R., Tchieu, J., Mason, M.J., Yachechko, R., Kuoy, E., Horvath, S., Zhou, Q., and Plath, K. (2009). Role of the murine reprogramming factors in the induction of pluripotency. Cell *136*, 364–377.

Takahashi, K., and Yamanaka, S. (2006). Induction of pluripotent stem cells from mouse embryonic and adult fibroblast cultures by defined factors. Cell *126*, 663–676.

Utikal, J., Polo, J.M., Stadtfeld, M., Maherali, N., Kulalert, W., Walsh, R.M., Khalil, A., Rheinwald, J.G., and Hochedlinger, K. (2009). Immortalization eliminates a roadblock during cellular reprogramming into iPS cells. Nature *460*, 1145–1148.

Wang, E.S., Reyes, N.A., Melton, C., Huskey, N.E., Momcilovic, O., Goga, A., Blelloch, R., and Oakes, S.A. (2015). Fas-activated mitochondrial apoptosis culls stalled embryonic stem cells to promote differentiation. Curr. Biol. *25*, 3110–3118.

Willis, S.N., Fletcher, J.I., Kaufmann, T., van Delft, M.F., Chen, L., Czabotar, P.E., Ierino, H., Lee, E.F., Fairlie, W.D., Bouillet, P., et al. (2007). Apoptosis initiated when BH3 ligands engage multiple Bcl-2 homologs, not Bax or Bak. Science *315*, 856–859.

Young, M.A., Larson, D.E., Sun, C.W., George, D.R., Ding, L., Miller, C.A., Lin, L., Pawlik, K.M., Chen, K., Fan, X., et al. (2012). Background mutations in parental cells account for most of the genetic heterogeneity of induced pluripotent stem cells. Cell Stem Cell *10*, 570–582.

Stem Cell Reports, Volume *10*

Supplemental Information

BAK/BAX-Mediated Apoptosis Is a *Myc*-Induced Roadblock to Reprogramming

Esther J.Y. Kim, Minna-Liisa Anko, Christoffer Flensberg, Ian J. Majewski, Fan-Suo Geng, Jaber Firas, David C.S. Huang, Mark F. van Delft, and Joan K. Heath

Stem Cell Reports, Volume 10

Supplemental Information

BAK/BAX-Mediated Apoptosis is a *Myc*-Induced Roadblock to Reprogramming

Esther J. Y. Kim, Minna-Liisa Anko, Christoffer Flensberg, Ian J. Majewski, Fan-Suo Geng, Jaber Firas, David C. S. Huang, Mark F. van Delft and Joan K. Heath

Supplemental Information comprises:

Figure S1

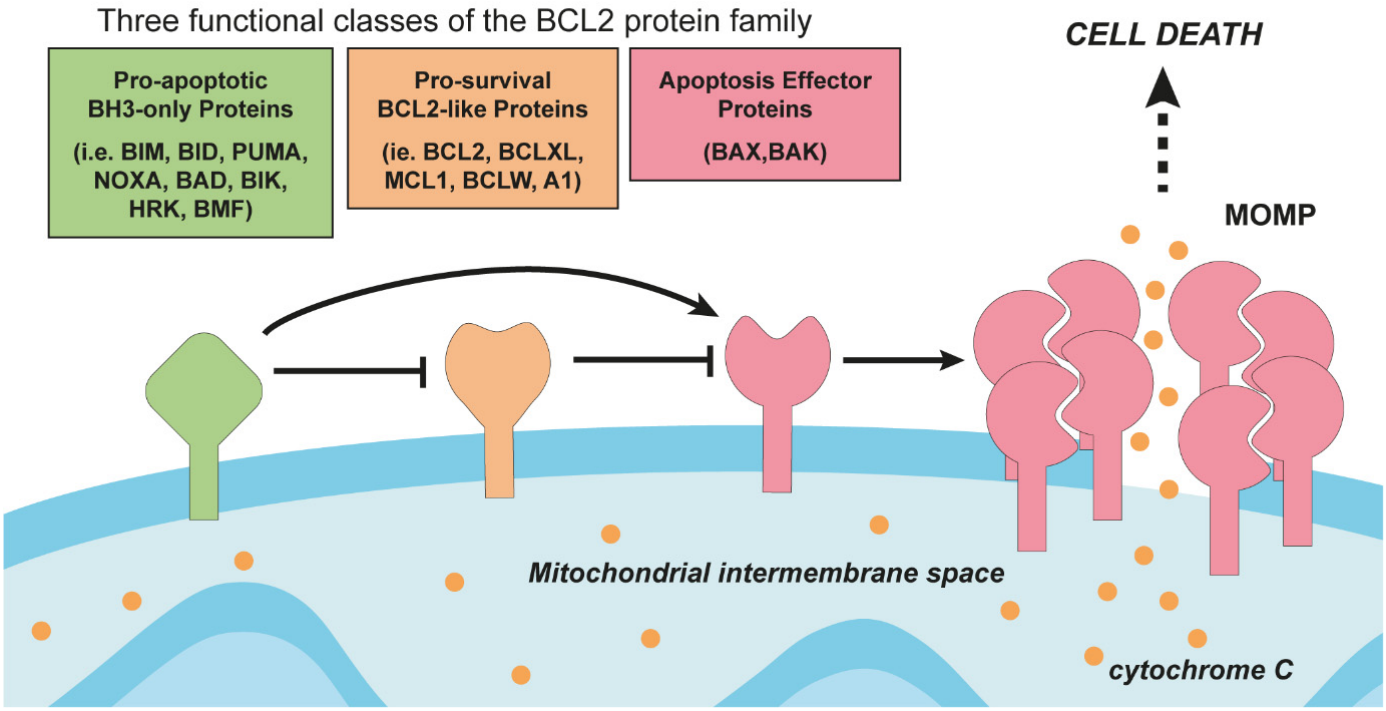
Three functional classes of the BCL2 protein family
Pro-apoptotic BH3-only Proteins
(i.e. BIM, BID, PUMA, NOXA, BAD, BIK, HRK, BMF)
Pro-survival BCL2-like Proteins
(ie. BCL2, BCLXL, MCL1, BCLW, A1)
Apoptosis Effector Proteins
(BAX,BAK)
CELL DEATH
MOMP
Mitochondrial intermembrane space
cytochrome C

Figure S2

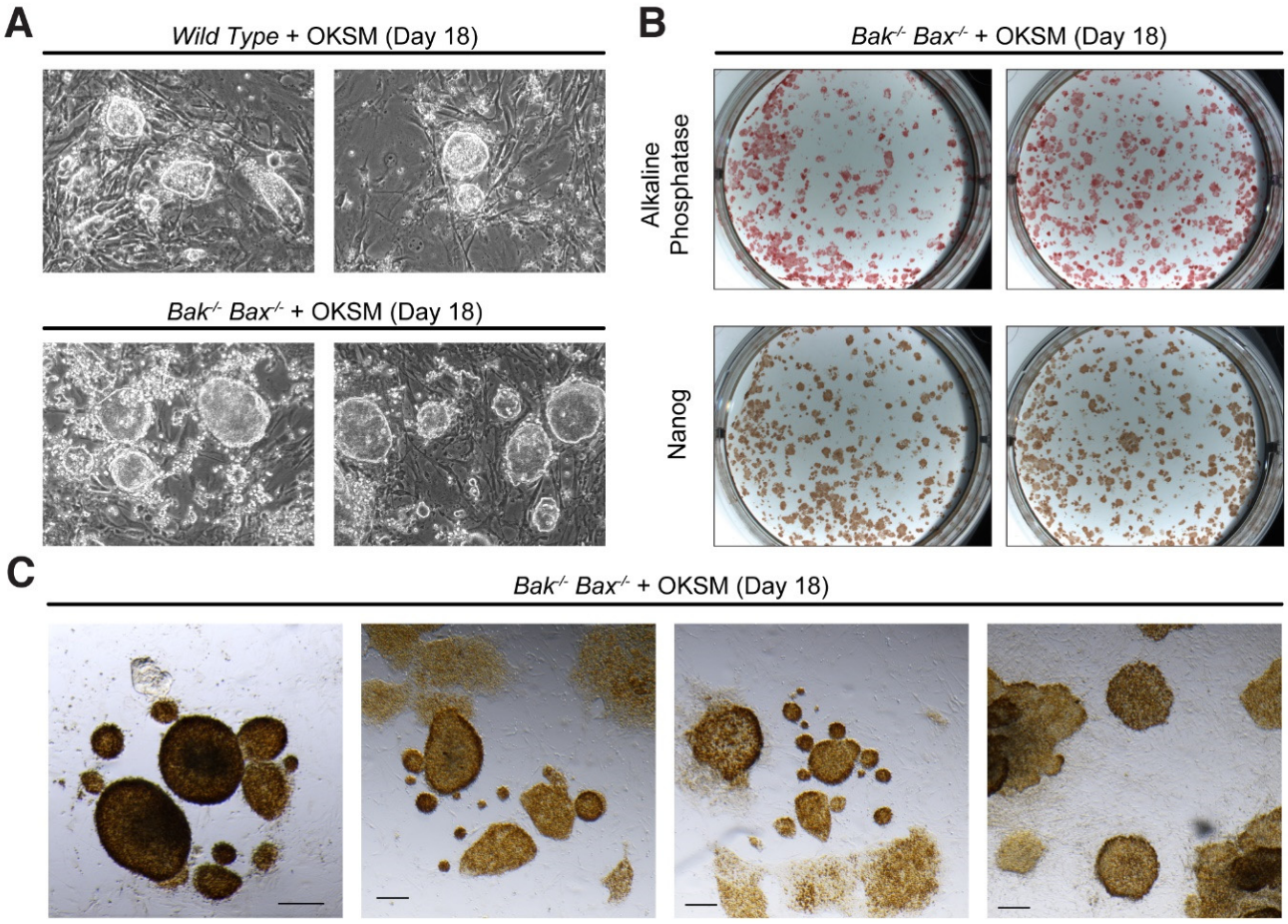
A
Wild Type + OKSM (Day 18)
Bak-/- Bax-/- + OKSM (Day 18)
B
Bak-/- Bax-/- + OKSM (Day 18)
Alkaline Phosphatase
Nanog
C
Bak-/- Bax-/- + OKSM (Day 18)

Figure S3A

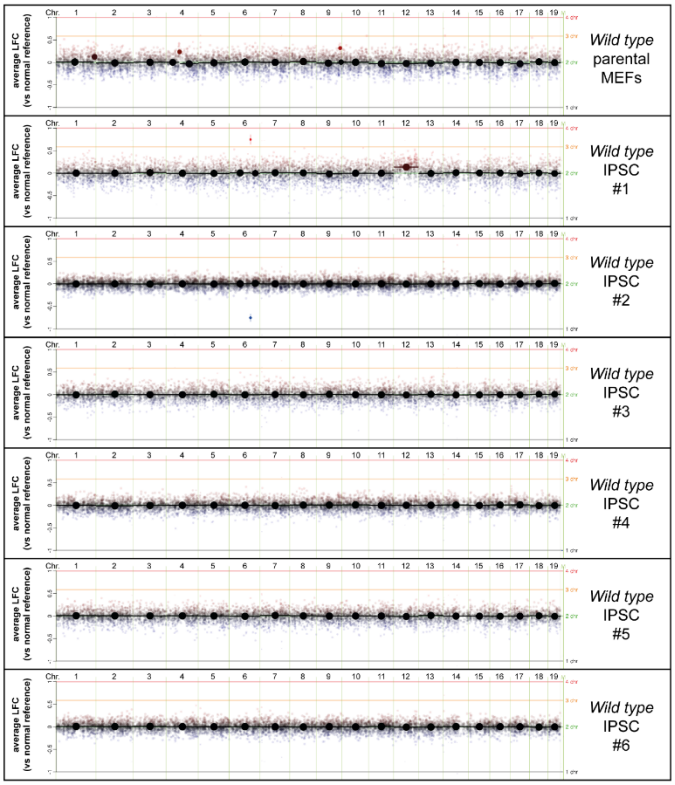

Figure S3B

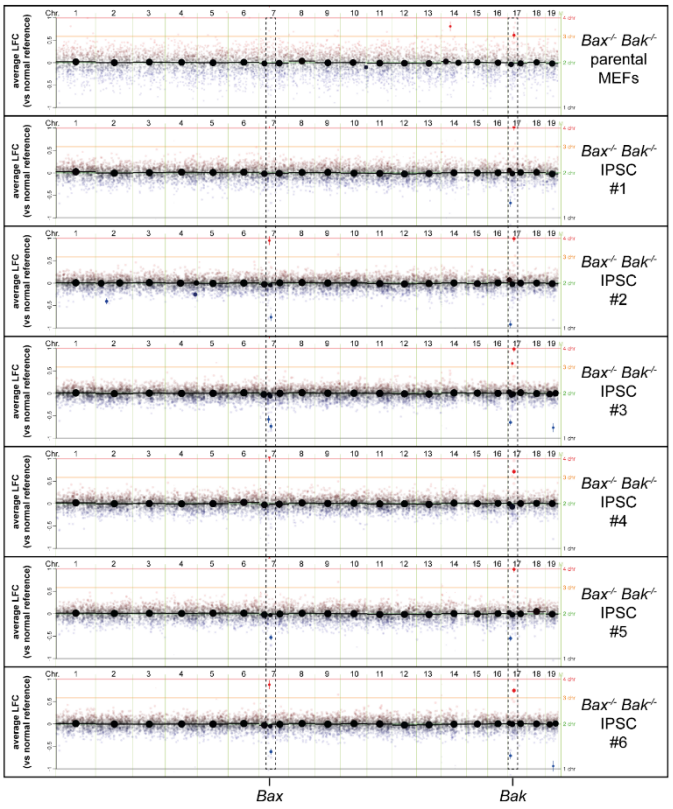

Figure S3C

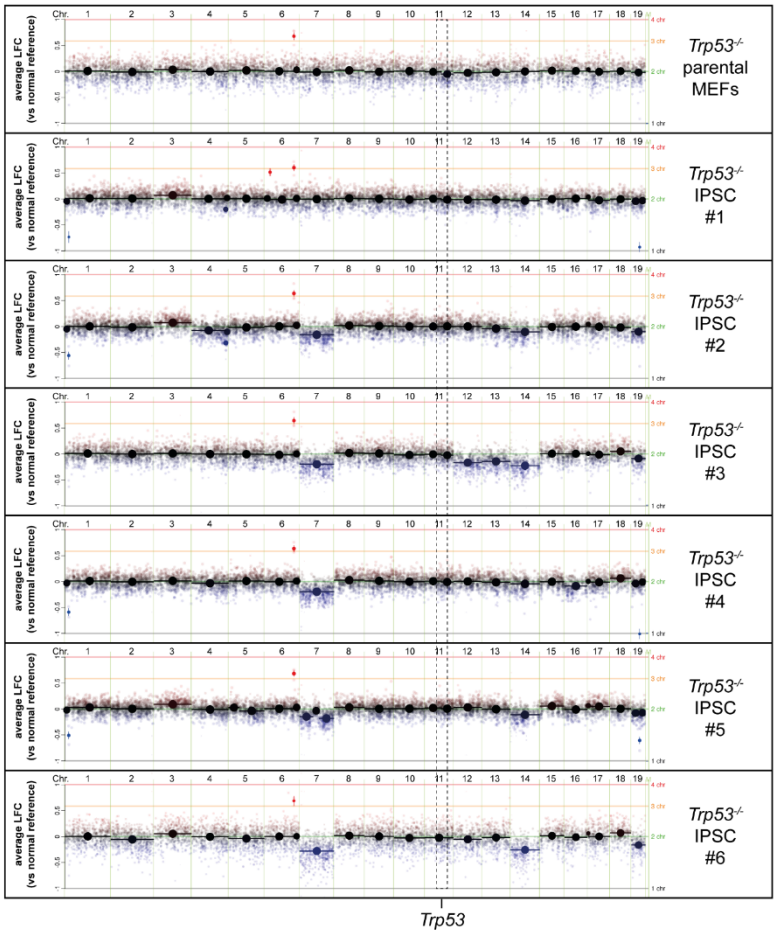

SUPPLEMENTAL FIGURE TITLES AND LEGENDS

Figure S1. Regulation of mitochondrial apoptosis by the BCL2 family of proteins (related to Introduction). In healthy cells, BCL2-like proteins (BCL2, BCLXL, BCLW, MCL1, A1) restrain the apoptosis effector proteins BAK and BAX to permit cell survival. During apoptosis, BH3-only proteins (BIM, BID, BAD, PUMA, NOXA, BMF, BIK, HRK) become activated by stress signals and prevent BCL2-like proteins from inhibiting BAK and BAX. Some BH3-only proteins (e.g. BIM, BID) also activate BAK and BAX directly. Once active, BAK and BAX form dimers that assemble into higher order oligomers, which cause mitochondrial outer membrane permeabilization (MOMP). This leads to the efflux of cytochrome c to the cytosol where it activates caspase proteases, leading to the demolition of cellular components and cell death.

Figure S2. iPSC Morphology and Marker Expression (related to Figure 1). (**A**) MEFs transduced with OKSM yielded shiny, rounded colonies characteristic of pluripotent stem cells. The morphology of iPSC colonies is comparable between *WT* and *Bak*$^{-/-}$*;Bax*$^{-/-}$ cultures. (**B**) *Bak*$^{-/-}$;*Bax*$^{-/-}$ MEFs transduced with OKSM in duplicate wells were cultured for 18 d and then fixed and stained. One replicate well was stained with Vector Red Alkaline Phosphatase substrate. The other was stained with anti-NANOG primary antibody, which was detected with an HRP-conjugated secondary antibody and Vector DAB peroxidase substrate. Duplicate wells from two independent *Bak*$^{-/-}$;*Bax*$^{-/-}$ MEF clones are shown. **(C)** Higher magnification images of reprogrammed *Bak*$^{-/-}$;*Bax*$^{-/-}$ MEFs stained for NANOG protein (brown) reveal cells at different stages of reprogramming, as well as unstained cells that failed to be reprogrammed. Scale bar = 200μm.

Figure S3. Genomic Integrity of *Bak*$^{-/-}$;*Bax*$^{-/-}$ iPSCs is Comparable to *WT* iPSCs (related to Figure 4). Segmented copy number data are shown for each sample. The log fold change (LFC) is plotted for each 100kb interval, relative to the *WT* reference set. The chromosome number is listed at the top of each panel. Each segment is denoted by a point with a horizontal line extending over the length of the segment and a colour gradient that reflects the copy number status (blue for loss, red for gain and black for unchanged). Error bars represent 70% confidence intervals. Individual sample names are listed (at right). (**A, B**) Very few copy number alterations (CNAs) were detected in passage 2 *WT* and *Bak*$^{-/-}$;*Bax*$^{-/-}$ iPSCs, apart from several small variations (<100kb) found in close proximity to the targeted alleles in *Bak*$^{-/-}$;*Bax*$^{-/-}$ iPSCs (i.e. *Bak*, *Bax* on chromosomes 17 and 7, respectively). These were also detected in the parental MEFs and do not reflect CNAs arising during the reprogramming process. Instead, they reflect strain-specific variations from the reference C57BL/6 genome linked to the *Bax* and *Bak* loci, which have been maintained despite extensive backcrossing (N.B. the *Bax*$^{-/-}$ and *Bak*$^{-/-}$ alleles were originally established on a 129/Sv background). Detection of these events indicates that the low pass whole genome sequencing we conducted was sensitive and that most of the spontaneous CNAs observed in the iPSC lines were sub-clonal. (**C**) The genomes of iPSCs derived from p53-deficient MEFs harboured a significantly higher number of CNAs, consistent with many previous reports that iPSCs derived from p53-deficient MEFs exhibit elevated genome instability.

SUPPLEMENTAL TABLES

Table S1. Primary antibodies used in this study

PRIMARY ANTIBODY	WORKING DILUTION	SUPPLIER	CATALOGUE NUMBER
Mouse monoclonal anti-OCT3/4	1:100	Santa Cruz	sc-5279
Rabbit polyclonal anti NANOG	1:150	Abcam	ab-80892
Mouse monoclonal anti-SSEA1	1:800	Cell Signaling Technology	4744
Rabbit polyclonal anti-α1-Fetoprotein	1:200	Dako	A0008
Mouse monoclonal anti-βIII Tubulin	1:1000	Promega	G7121
Mouse monoclonal anti-α Smooth Muscle Actin	1:400	Sigma	2547
Mouse monoclonal anti-p53	1:500	BD Pharmingen	554147
Mouse Monoclonal anti-phospho (γ) H2A-X	1:500	Merck Millipore	05-636

Table S2. Secondary antibodies used in this study

SECONDARY ANTIBODY	WORKING DILUTION	SUPPLIER	CATALOGUE NUMBER
Mouse anti-rabbit IgG FITC (H+L chain specific)	1:200	Southern Biotech	4050-02
Goat anti-mouse IgG PE (H+L chain specific)	1:200	Southern Biotech	1031-09

SUPPLEMENTAL EXPERIMENTAL PROCEDURES

Generation of Mouse iPSCs

Primary MEFs at passage 3-4 were seeded onto 6-well plates (5 x 10^4 cells per well) pre-coated with 0.1% gelatin. These were transduced by centrifuging (45 min, 1100x*g*) with the lentiviral supernatant followed by overnight incubation. Transduced cells were cultured in iPSC medium (15% Knockout Serum Replacement, 2mM GlutaMAX-CTS, 1mM non-essential amino acids, 1000U/ml leukemia inhibitory factor (LIF), 100μM β-mercaptoethanol in Knockout DMEM) for 18 d. Media was changed every 48 h. On day 18 reprogramming efficiency was assessed using the Vector Red Alkaline Phosphatase Substrate Kit according to the manufacturer's instructions, or by NANOG immunocytochemistry (see Tables S1, S2). The high magnification images of NANOG staining were acquired with a SMZ25 stereomicroscope (Nikon) and DS-Ri2 high definition colour camera (Nikon).

Teratoma Formation

1 x 10^6 cells of each iPSC clone were subcutaneously injected into NOD/SCID mice. Teratomas were surgically removed 4-5 weeks post-injection. Tissues were fixed overnight at 4°C in 4% paraformaldehyde and embedded in paraffin. 2-3 μm sections were taken from samples and stained with hematoxylin and eosin for pathological examination.

Immunofluorescence

The primary and secondary antibodies used in this study are described in Tables S1 and S2. iPSC clones were fixed with 4% PFA for 10 min, permeabilized with 0.1% Triton X-100 for 10 min, and blocked with 2% BSA in PBS for 1 h at room temperature (R.T). After incubation with antibodies against mouse SSEA1, NANOG, OCT4 or p53 overnight at 4°C, cells were washed with PBS with 0.1% Tween 20 and incubated either with secondary

antibodies conjugated with R-phycoerythrin or FITC for 1 h at R.T. For SSEA1 staining, the permeabilization step was not necessary. Washed coverslips were mounted on slides with Prolong Gold Antifade Reagent (Invitrogen) with DAPI. Images were acquired under non-saturating conditions on a Zeiss LSM 780 confocal microscope.

In Vitro Differentiation Assay

iPSCs were harvested and re-suspended at a concentration of 2.5 x 10^4 cells/ml in iPSC medium without LIF. Hanging droplets (20 µl) were made on the underside of a 9 cm cell culture plate lid, incubated for 2 d and then transferred to non-adhesive plates and cultured in suspension for 3 d to form embryoid bodies (EBs). EBs were then transferred to gelatin-coated tissue culture plates to differentiate for 9 - 14 d. Cells were stained for α-smooth muscle actin, βIII tubulin and α fetoprotein, along with DAPI.

Detection of DNA Double-Strand Breaks

DNA double-strand breaks were detected by immunofluorescence using a primary antibody against mouse H2AX (Table S1). Fluorescence intensity threshold was set by a positive control of *WT* iPSC colonies treated with 5 Gray of γ-irradiation. Foci in 100-150 nuclei per genotype per experiment were counted. DNA double-strand breaks were quantified automatically with Image J based on thresholds set by positive controls.

Image Analysis

All images were analysed with the Fiji image processing package.

Western Blot Analysis

MEFs were treated with doxorubicin (0.5µg/ml) for 18 h to increase p53 levels and protein extracts were prepared by lysis in RIPA buffer supplemented with protease inhibitors

(Roche). Proteins were quantified using the Bradford assay (Bio-Rad), separated by SDS-PAGE and transferred to a nitrocellulose membrane. After blocking with 5% (w/v) skimmed milk powder in PBS-Tween20 (0.1%), the membrane was incubated with primary antibody against p53 (Table S1).